Non-Hermitian quantum Fermi accelerator

Andreas Fring [1,*] and Takano Taira [2,†]
[1] Department of Mathematics, City, University of London, Northampton Square, London EC1V 0HB, England
[2] Research Fellow of Japan Society for the Promotion of Science, Institute of Industrial Science, The University of Tokyo, 5-1-5 Kashiwanoha, Kashiwa 277-8574, Japan

(Received 22 April 2023; accepted 12 July 2023; published 31 July 2023)

We exactly solve a quantum Fermi accelerator model consisting of a time-independent non-Hermitian Hamiltonian with time-dependent Dirichlet boundary conditions. A Hilbert space for such systems can be defined in two equivalent ways, either by first constructing a time-independent Dyson map and subsequently unitarily mapping to fixed boundary conditions or by first unitarily mapping to fixed boundary conditions followed by the construction of a time-dependent Dyson map. In turn, this allows to construct time-dependent metric operators from a time-independent metric and two time-dependent unitary maps that freeze the moving boundaries. From the time-dependent energy spectrum, we find the known possibility of oscillatory behavior in the average energy in the $\mathcal{PT}$ regime, whereas in the spontaneously broken $\mathcal{PT}$ regime we observe the feature of a one-time depletion of the energy. We show that the $\mathcal{PT}$ broken regime is mended with a moving boundary, equivalently to mending it with a time-dependent Dyson map.

DOI: 10.1103/PhysRevA.108.012222

I. INTRODUCTION

Classical versions of Fermi accelerators were originally proposed by Fermi [1] more than seventy years ago as a possible explanation for the high energies observed in cosmic radiation. The simplest classical Fermi accelerator model consists of a free particle moving between two walls simulating magnetic fields, with one of them fixed and the other moving in time, with the collisions between the particle and the walls being perfectly elastic. In addtion to predicting features of cosmic rays in the spirit of the original motivation, such as the maximum energy that particles can reach is proportional to the strength of the magnetic field and the size of the acceleration region, the models were also found to exhibit classical chaotic behavior [2–4]. The chaotic behavior is due to the fact that the description in phase space of consecutive scatterings between the walls and the particle leads to nonlinear maps, which in their simplest version, correspond to the so-called Ulam maps. For a recent overview of the latest experimental observations of ultrahigh energy cosmic rays, see, for instance [5].

Quantum versions of Fermi accelerator models are set up in a similar fashion, described by the Schrödinger equation with Dirichlet boundary conditions. They allow us to study quantum chaos [6,7] and other interesting phenomena [8–13], such as the possibility of an energy gain in the time-dependent spectrum. Here the purpose is to investigate such a system with the starting Hamiltonian taken to be non-Hermitian, but $\mathcal{PT}$-symmetric or pseudo-Hermitian. In the broken $\mathcal{PT}$ regime we observe the previously unseen nonperiodic nature of the average energy over time.

Our starting point is to consider a time-independent $\mathcal{PT}$-symmetric or pseudo-Hermitian [14,15] Hamiltonian $\tilde{H} = -\frac{\hbar^2}{2m}\partial_x^2 + \tilde{V}(x)$, where $\tilde{V}(x)$ is a non-Hermitian potential. The Schrödinger equation with Dirichlet boundary condition is given by

$$i\hbar\frac{\partial}{\partial t}\tilde{\psi}(t,x) = \tilde{H}(x)\tilde{\psi}(t,x), \quad \tilde{\psi}(t,\pm\ell) = 0, \qquad (1)$$

where $\ell > 0$. The Hilbert space of the system consists of square-integrable functions in the interval $[-\ell,\ell]$, i.e., $\tilde{\psi}(t,x) \in L^2([-\ell,\ell])$. This Hamiltonian is said to be $\mathcal{PT}$ symmetric if the Hamiltonian and the wave functions are symmetric under an antilinear transformation, such as $p \to p$, $x \to -x$, and $i \to -i$, in our case.

The standard procedure in $\mathcal{PT}$-symmetric quantum mechanics is to map the non-Hermitian Hamiltonian (1) to a Hermitian Hamiltonian with a Dyson map η such that $\tilde{H} = \eta\tilde{h}\tilde{\eta}^{-1} \neq \tilde{H}^\dagger, \tilde{h}^\dagger = \tilde{h}$. Recall that the Dyson map η is generally nonunique. Extensive discussion on the uniqueness of η can already be found in [16], where the authors demonstrated that η was uniquely fixed by demanding the irreducibility of some set of operators. In the case of the Swanson model [17], it was equivalently shown in [18] that the uniqueness of η can be ensured by requiring the Hamiltonian and one other operator (e.g., position, momentum, or number operator) to correspond to their Hermitian counterpart.

Let us denote the new wave function $\tilde{\phi}(t,x) = \tilde{\eta}\tilde{\psi}(t,x)$ where the non-Hermitian operator $\tilde{\eta}$ is time independent. Therefore, the Schrödinger equation and the boundary condition (1) are simply mapped to

$$i\hbar\frac{d}{dt}\tilde{\phi}(t,x) = \tilde{h}(x)\tilde{\phi}(t,x), \quad \tilde{\phi}(t,\pm\ell) = 0. \qquad (2)$$

*a.fring@city.ac.uk
†taira904@iis.u-tokyo.ac.jp

TABLE I. The average energy $\langle E\rangle_\eta$ defined in Eq. (3) is compared for two $\mathcal{PT}$ regimes with time-dependent or independent boundary conditions. In both cases there is a phase transition in the dynamical behavior of $\langle E\rangle_\eta$ between $\mathcal{PT}$ broken or unbroken regimes. The detail is presented in Sec. III.

	$\mathcal{PT}$ symmetric	$\mathcal{PT}$ broken
Time-independent boundary	$\langle E\rangle_\eta \in \mathbb{R}$	$\langle E\rangle_\eta \in \mathbb{C}$
Time-dependent boundary	$\langle E\rangle_\eta \in \mathbb{R}$	$\langle E\rangle_\eta \in \mathbb{R}$

In $\mathcal{PT}$-symmetric quantum mechanics the inner product in the Hilbert space needs to be redefined. Accordingly, the average energy of the non-Hermitian Hamiltonian is given by $\langle E\rangle_\eta =: \int_{-\ell}^{\ell} dx \tilde{\psi}\tilde{\rho}\tilde{H}\tilde{\psi}$, where the Hermitian positive-definite metric is defined as $\tilde{\rho} := \tilde{\eta}^\dagger\tilde{\eta}$. This can be rewritten in terms of the Hermitian Hamiltonian as

$$\langle E(t)\rangle_\eta := \int_{-\ell}^{\ell} dx\tilde{\psi}^\dagger\tilde{\rho}\tilde{H}\tilde{\psi} = \int_{-\ell}^{\ell} dx\tilde{\phi}^\dagger\tilde{h}\tilde{\phi}. \quad (3)$$

The common characteristic of the non-Hermitian system is that the above equality only holds when the non-Hermitian Hamiltonian and the wave function are $\mathcal{PT}$ symmetric. The average energy of $\tilde{H}$ acquires complex conjugate eigenvalues in the $\mathcal{PT}$-broken regime. However, we will show that when the boundary ℓ is time dependent, the average energy is defined above the square real energy, even in the $\mathcal{PT}$-broken regime.

It was established that real-valued average energies can be obtained in all regimes when the non-Hermitian Hamiltonian or the Dyson map are time dependent [19]. See also the review of the time-dependent non-Hermitian quantum mechanics [20]. In this work, we demonstrate that real-valued average energies can also be attained in the $\mathcal{PT}$-broken regime of the Swanson model by introducing time dependence to the boundary condition ℓ, instead of the Hamiltonian or Dyson map. Moreover, we establish the equivalence of our approach with a previous method [19], where the Dyson map's time dependence was used to mend the $\mathcal{PT}$-broken regime. Our two primary findings are summarized in Table I and Fig. 1. We will provide the explicit derivation of the scheme in Fig. 1 in the next section.

II. EQUIVALENCE OF TIME-DEPENDENT BOUNDARY AND DYSON MAP

Let us assume that the boundary is time dependent, i.e., $\ell = \ell(t)$, then, the wave functions $\tilde{\psi}(t,x)$ and $\tilde{\psi}(t',x)$ belong to two different Hilbert spaces for $t \neq t'$. Therefore, the time derivative of the wave function does not belong to any Hilbert space for any time slice, which implies that the above Schrödinger equation is not well defined. However, in [21], the problem was resolved by formally embedding the system into a larger domain $L^2(\mathbb{R}) = L^2([-\ell,\ell]) \otimes L^2((-\infty,-\ell) \cup (\ell,\infty))$, where extended Hamiltonian is $\tilde{H}(x) \oplus 0$. This embedding implies that the integration contour of the average energy (3) can be understood as

$$\langle E(t)\rangle_\eta = \int_{-\infty}^{\infty} dx\tilde{\psi}^\dagger\tilde{\rho}[\tilde{H}(x) \oplus 0]\tilde{\psi} = \int_{-\ell(t)}^{\ell(t)} dx\tilde{\psi}^\dagger\tilde{\rho}[\tilde{H}(x)]\tilde{\psi}. \quad (4)$$

To remove the time dependence of the boundary from the Hilbert space, a time-dependent unitary operator $U(t)$ is introduced as

$$U : L^2(\mathbb{R}) \to L^2(\mathbb{R}), \quad f(t,x) \to \sqrt{\ell(t)} f(t,\ell(t)x), \quad (5)$$

which maps all wave functions in $L^2(\mathbb{R})$ to $L^2(\mathbb{R}) = L^2([-1,1]) \otimes L^2((-\infty,-1) \cup (1,\infty))$, thereby removing the time dependence of the boundary from the Hilbert space. The factor $\sqrt{l(t)}$ is necessary to ensure the transformation is unitary. The Hamiltonian is mapped to $U\tilde{H}U^\dagger \oplus 0$. For the

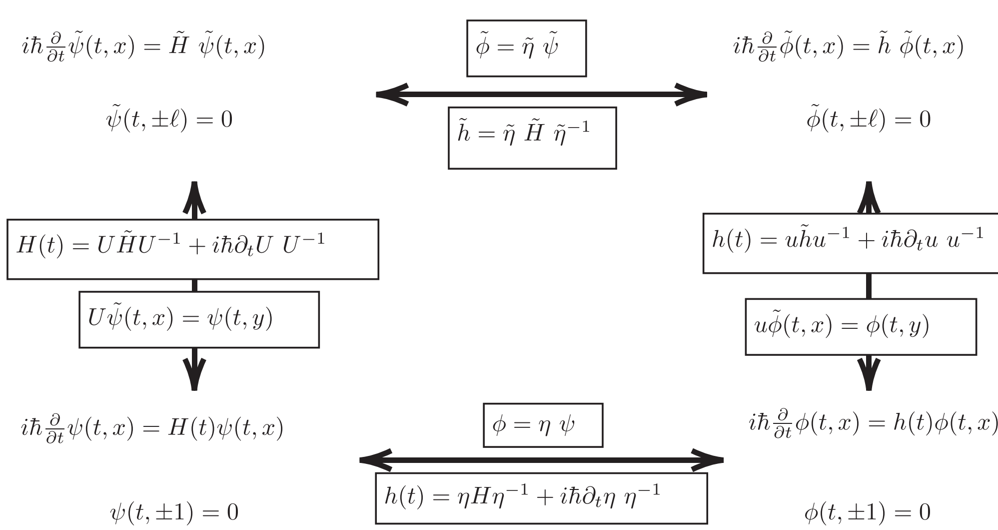

FIG. 1. Commutative scheme, showing the relations between two time-independent Schrödinger equations with time-dependent boundary conditions on the top row and two time-dependent Schrödinger equations with time-independent boundary conditions on the bottom row.

rest of the paper, we will drop the 0 component of the extended operators for brevity.

Let us define the unitary transformed wave function as $U(t)\tilde{\psi}(t,x) =: \psi(t,x)$. The time-dependent Schrödinger equation (1) is also mapped by the unitary operator as

$$i\hbar\frac{\partial}{\partial t}\psi(t,y) = (U\tilde{H}(x)U^\dagger + i\hbar U\partial_t U^\dagger)\psi(t,y) = \left[\tilde{H}(y) + \frac{\partial_t \ell}{2\ell}\{y, i\hbar\partial_y\}\right]\psi(t,y) =: H(t,y)\psi(t,y), \tag{6}$$

where $y = \ell x \in [-1, 1]$.

Alternatively, assuming pseudo-Hermiticity, the time-independent non-Hermitian Hamiltonian (1) can be mapped to a Hermitian Hamiltonian via the Dyson map $\tilde{H} = \eta\tilde{h}\tilde{\eta}^{-1}$, $\tilde{h}^\dagger = \tilde{h}$. Note that when we consider the $\mathcal{PT}$-broken regime, the pseudo-Hermicity is broken and the Hamiltonian $\tilde{h}$ becomes non-Hermitian. However, we will show that even in such a case, the average energy (3) is real due to the time-dependent boundary. Let us denote the new wave function $\tilde{\phi}(t,x) := \tilde{\eta}\tilde{\psi}(t,x)$ where the non-Hermitian operator $\tilde{\eta}$ is time independent. Therefore, the Schrödinger equation and the boundary conditions (1) are simply mapped to

$$i\hbar\frac{d}{dt}\tilde{\phi}(t,x) = \tilde{h}(x)\tilde{\phi}(t,x), \quad \tilde{\phi}(t,\pm\ell) = 0. \tag{7}$$

Then the above procedure to remove the boundary time dependence can be applied to the mapped Hermitian system, and we obtain

$$i\hbar\frac{d}{dt}\phi(t,y) = (u\tilde{h}u^\dagger - i\hbar u\partial_t u^\dagger)\phi(t,y) = \left[\tilde{h}(y) + \frac{\partial_t \ell}{2\ell}\{y, i\hbar\partial_y\}\right]\phi(t,y) = h(t)\phi(t,y), \tag{8}$$

where $u\tilde{\phi}(t,x) = \phi(t,y)$ and u is also defined in a same way as Eq. (5).

It has been shown that in the time-dependent case [22], the Dyson map between non-Hermitian and Hermitian operators is given by

$$H(t) := \eta(t)h(t)\eta(t)^{-1} + i\hbar\frac{\partial\eta}{\partial t}\eta^{-1}, \tag{9}$$

where the Dyson map $\eta(t)$ is a time-dependent non-Hermitian operator. We summarize the relation between Eqs. (1), (6), (7), and (8) in the Fig. 1. Note that by requiring the scheme in Fig. 1 to be commutative, we find the relation between two similarity transformations and the two Dyson maps

$$\eta(t) = u(t)\tilde{\eta}U^\dagger(t), \tag{10}$$

which leads to the equivalence between the non-Hermitian time-dependent boundary problem (1) and the non-Hermitian time-dependent Hamiltonian problem with a time-dependent metric (6) discussed in [19].

Once we obtain the time-dependent Hermitian Hamiltonian, the average energy (3) can be calculated. Using the relations in Fig. 1 and the Eq. (10), one can write down four alternative formulations of the average energy (3)

$$\langle E(t)\rangle = \int_{-\ell(t)}^{\ell(t)} dx\tilde{\psi}^\dagger\tilde{\rho}\tilde{H}\tilde{\psi} = \int_{-\ell(t)}^{\ell(t)} dx\tilde{\phi}^\dagger\tilde{h}\tilde{\phi} \tag{11}$$

$$= \int_{-1}^{1} dx\phi^\dagger(h - i\hbar u_t u^\dagger)\phi \tag{12}$$

$$= \int_{-1}^{1} dx\psi^\dagger\eta^\dagger\eta[H + i\hbar(u^\dagger\eta)^{-1}\partial_t(u^\dagger\eta)]\psi. \tag{13}$$

The operator inside the square brackets in Eq. (13) is called the energy operator. It was initially introduced in [22], serving as an isospectral operator in relation to the Hermitian operator procured through the time-dependent Dyson mapping of a non-Hermitian Hamiltonian. The implementation of this operator addresses the nonisospectral characteristic of the non-Hermitian Hamiltonian and its Hermitian counterpart, a discrepancy that arises due to the time dependence of the Dyson map.

We will apply these general relations to a specific example that we choose to be the Swanson model in the next section.

III. SWANSON MODEL: MENDING $\mathcal{PT}$-BROKEN REGIME VIA MOVING BOUNDARY

Typically, finding the exact Dyson map poses a substantial challenge, given that it necessitates solving an operator-valued algebraic equation. The Swanson model [17] is one of the rare cases wherein multiple metrics have been found [18], even in the time-dependent case [22]. Exploiting this characteristic, we will compute the average energy corresponding to three distinct metrics, showing the energy spectrum is, indeed, real in all three instances.

Furthermore, we will show that a time-dependent boundary can lead to the real average energy in both $\mathcal{PT}$-symmetric and broken regimes. Let us consider the Swanson Hamiltonian [17]

$$\tilde{H} = \frac{\omega_-}{2}p^2 + \frac{\omega_+}{2}x^2 + \frac{i}{2}\mathcal{A}\{x,p\}, \quad i\hbar\partial_t\tilde{\psi} = \tilde{H}\tilde{\psi}, \tag{14}$$

where $p = -i\hbar\partial_x$, $\omega_\pm := \omega \pm (\alpha+\beta)$, and $\mathcal{A} := \alpha - \beta$. According to [18], the Hamiltonian (14) can be mapped via a similarity transformation to a harmonic oscillator, which corresponds to the top-right corner of the commutative diagram in Fig. 1

$$\tilde{\eta}_i\tilde{H}\tilde{\eta}_i^{-1} = A_i(\alpha,\beta)p^2 + B_i(\alpha,\beta)x^2 =: \tilde{h}_i, \tag{15}$$

$$\tilde{\eta}_i\tilde{\psi} = \tilde{\phi}_i, \quad i\hbar\partial_t\tilde{\phi}_i = \tilde{h}_i\tilde{\phi}_i, \tag{16}$$

where the index i labels the nonunique choices of the Dyson maps. The specific forms of the parameters $A_i(\omega,\alpha,\beta)$ and $B_i(\omega,\alpha,\beta)$ are fixed by assuming at least two operators to be mapped to their Hermitian counterparts [16]. Below we list three examples taken from [18]

$$A_1 = \frac{\omega - 2\sqrt{\alpha\beta}}{2\omega}, \quad B_1 = \frac{\omega(\omega + 2\sqrt{\alpha\beta})}{2} : \tilde{\eta}_i H \tilde{\eta}_i^{-1} = \tilde{h}_i, \quad \tilde{\eta}_i N \tilde{\eta}_i^{-1} = N, \tag{17}$$

$$A_2 = \frac{\omega - \alpha - \beta}{2\omega}, \quad B_2 = \frac{\omega}{2}\frac{\omega^2 - 4\alpha\beta}{\omega - \alpha - \beta} : \tilde{\eta}_i H \tilde{\eta}_i^{-1} = \tilde{h}_i, \quad \tilde{\eta}_i x \tilde{\eta}_i^{-1} = x, \tag{18}$$

$$A_3 = \frac{\omega^2 - 4\alpha\beta}{2\omega(\omega + \alpha + \beta)}, \quad B_3 = \frac{\omega(\omega + \alpha + \beta)}{2} : \tilde{\eta}_i H \tilde{\eta}_i^{-1} = \tilde{h}_i, \quad \tilde{\eta}_i p \tilde{\eta}_i^{-1} = p, \tag{19}$$

where N is a number operator.

The average energy (3) of the Hamiltonian is computed to

$$\langle E \rangle = (n + 1/2)\sqrt{\omega^2 - 4\alpha\beta} = (n + 1/2)\sqrt{\mathcal{A}^2 + \omega_+\omega_-}$$

for $n \in \mathbb{N}$. The $\mathcal{PT}$ symmetry of the Swanson model is broken when $\omega^2 - 4\alpha\beta = \mathcal{A}^2 + \omega_+\omega_- < 0$. Therefore in the $\mathcal{PT}$-broken regime, the average energy becomes complex. This is a common feature of $\mathcal{PT}$-symmetry quantum mechanics. We will consider the time-dependent boundary to mend this complex energy analog to [19].

The Schrödinger equation (15) can be transformed by the unitary map (5) to give the time-dependent Hermitian Schrödinger equation $i\hbar\partial_t\phi_i = h\phi_i$ corresponding to the bottom right corner of the commutative diagram in Fig. 1. The explicit form of the time-dependent Hermitian Hamiltonian is

$$h_i(t, x) := \frac{\ell_t}{2\ell}\{x, i\hbar\partial_x\} - \frac{\hbar^2 A_i}{\ell^2}\partial_x^2 + B_i\ell^2 x^2, \tag{20}$$

for $i = 1, 2, 3$. The corresponding Schrödinger equation is simplified by performing a further unitary transformation of the form $\phi_j = c_1 \exp(i\frac{\ell\ell_t}{4A_j\hbar}x^2)\varphi_j(t, x)$, which reduces the equation to

$$0 = i4\hbar A_j \ell^2(\varphi_j)_t + \hbar^2 4A_j^2(\varphi_j)_{yy} - \ell^3(4A_jB_j\ell + \ell_{tt})y^2\varphi_j, \tag{21}$$

with c_j denoting the normalization constant. It is useful to notice that the combination of two parameters $4A_jB_j = \omega^2 - 4\alpha\beta =: \Omega$ takes the same form for all three examples (17) to (19).

The above equation can be reduced further into the effective Harmonic oscillator if we consider the solution to the equation $\ell^3(\Omega\ell + \ell_{tt}) = \kappa^2$ where κ is some constant. This is an Ermakov-Pinney equation [23,24], which can be solved exactly. One of the solutions is

$$\ell_j^2(t) = \frac{\kappa}{A_jB_j}\sin^2(2\sqrt{A_jB_j}t) + \kappa\cos^2(2\sqrt{A_jB_j}t) + \frac{2(\kappa - 1/4)}{\sqrt{A_jB_j}}\sin(2\sqrt{A_jB_j}t)\cos(2\sqrt{A_jB_j}t). \tag{22}$$

Introducing the new time variable $\tau = \int^t 1/\ell^2$, we find the effective Harmonic oscillator

$$i4\hbar A_j(\varphi_j)_\tau + \hbar^2 4A_j^2(\varphi_j)_{yy} - \kappa^2 y^2\varphi_j = 0. \tag{23}$$

Let us consider the ansatz $\varphi_j^n = \exp(-i\epsilon_j^n\tau_j/A_j\hbar)\chi_j^n(y)$. Then the above effective harmonic oscillator is reduced to a Sturm-Liouville eigenvalue problem

$$-\partial_{yy}\chi_j^n + \frac{\kappa^2}{4\hbar^2 A_j^2}y^2\chi_j^n = \epsilon_j^n\chi_j^n. \tag{24}$$

where there exist odd and even solutions that are given in terms of hypergeometric functions

$$\chi_{\mathrm{odd}}{}_j^n(y) = e^{-\frac{1}{2}\frac{\kappa y^2}{2\hbar A_j}}\left(\frac{\sqrt{\kappa}y}{\sqrt{2\hbar A_j}}\right){}_1F_1\left[\frac{3}{4} - \frac{1}{4}\frac{2\hbar A_j}{\kappa}\epsilon_j^n, \frac{3}{2}, \frac{\kappa y^2}{2\hbar A_j}\right],$$

$$\chi_{\mathrm{even}}{}_j^n(y) = e^{\frac{1}{2}\frac{\kappa y^2}{2\hbar A_j}}{}_1F_1\left[\frac{1}{4} + \frac{1}{4}\frac{2\hbar A_j}{\kappa}\epsilon_j^n, \frac{1}{2}, \frac{-\kappa y^2}{2\hbar A_j}\right].$$

Therefore, we find the solution to the effective Schrödinger equation corresponding to the bottom right corner of the commutative diagram shown in Fig. 1

$$\phi_j^n(t, x) = c_n^j e^{i\frac{\ell\ell_t}{4A_j\hbar}x^2 - i\frac{1}{A_j\hbar}\epsilon_j^n\tau_j}\chi_j^n(x), \tag{25}$$

where the constants c_n^j are fixed by the normalization $1 = \langle\phi_j^n|\phi_j^n\rangle \Rightarrow c_n^{-2} = \int_{-1}^1 dy\chi_n^\dagger\chi_n$.

The solution (25) can be mapped back to $\tilde{\phi}$ by use of an inverse mapping with the unitary transformation $u^\dagger\phi(t, x) = \phi[t, x/\ell(t)]/\sqrt{\ell(t)}$, which gives

$$\tilde{\phi}_j^n(t, x) = \frac{c_n^j}{\sqrt{\ell(t)}}e^{i\frac{\ell\ell_t}{4A_j\hbar}(\frac{x}{\ell(t)})^2 - i\frac{1}{A_j\hbar}\epsilon_j^n\tau_j}\chi_j^n[x/\ell(t)]. \tag{26}$$

Using this solution together with the Hamiltonian (15), one can calculate the average energy (11).

Average energy

The quantum Fermi accelerator commonly refers to the quantum harmonic oscillator with a time-dependent boundary condition. It was first introduced in [25] and one of its characteristics is its infinite increase of the average energy over time [7]. It was later shown that with some specific oscillation of the boundary condition [11], the average energy shows periodic gain and loss but zero net increase. We will show in this section that in the $\mathcal{PT}$-symmetric case, the behavior of the average energy coincides with the result of [11], and in the $\mathcal{PT}$-broken case, we observe an alternative behavior of the average energy where the periodicity of the average is lost.

Let us plot the average energy (11) for three different Dyson maps (17) to (19) in the $\mathcal{PT}$-symmetric ($\Omega > 0$) and the $\mathcal{PT}$-broken ($\Omega < 0$) regimes.

In the $\mathcal{PT}$-symmetric regime shown in Figs. 2(a) and 2(b), the average energy exhibits the periodic structure with $T = n\pi/2\sqrt{A_jB_j}$, $n \in \mathbb{Z}$ for all three metrics (17) to (19). This is because the average energy's periodicity is inherited from the boundary function (22), where the combination A_iB_i is equal for all metrics. This finding leads us to the same conclusion as in [11], indicating that although the average energy experiences time-dependent fluctuations, it remains periodic with no net gain or loss over a long time.

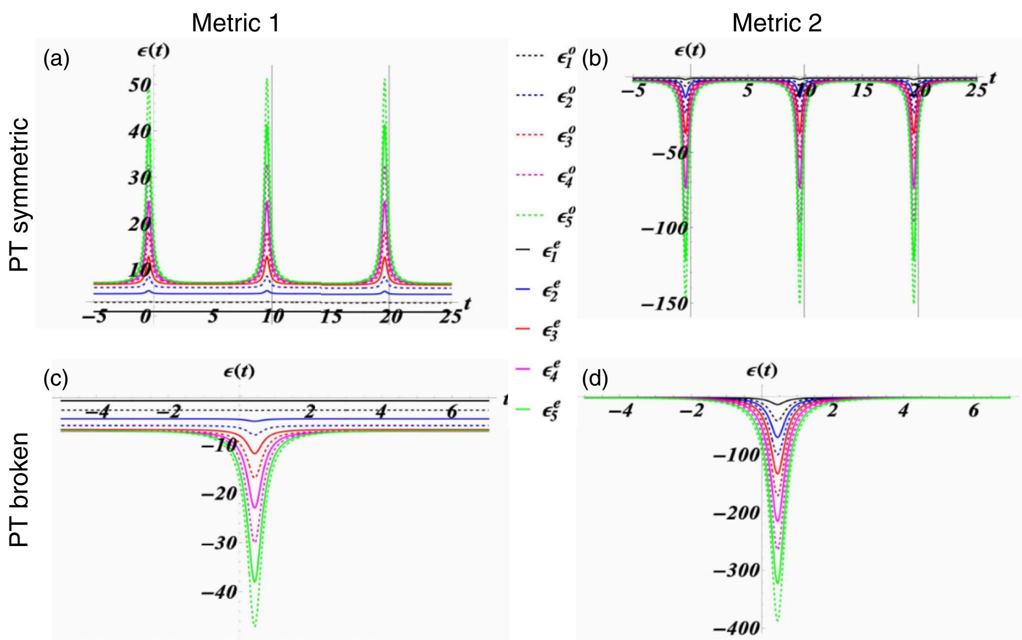

FIG. 2. Average energy for the $\mathcal{PT}$-symmetric or broken regimes over time for the first metric (17) in panels (a) and (c), respectively. The results computed with the second metric (18) for $\mathcal{PT}$-symmetric or broken regimes are shown in panels (b) and (d), respectively. The case involving the third metric (19) is omitted as it is almost identical to the first metric with a slight scale difference.

In the $\mathcal{PT}$-broken regime, the real-valued average energy is consistent with previous observations [19]. In Figs. 2(c) and 2(d), we observe an alternative behavior of the quantum Fermi accelerator, where the average energy loses its periodic structure in this regime due to the nonperiodic behavior of the boundary function (22), which hyperbolically diverges with time. Despite the divergent nature of the boundary function, the average energy remains constant over time and only experiences gain and loss near the origin.

Furthermore, we observe an alternative behavior of the non-Hermitian system where the probability density is infinitely spreading as the boundary moves away, which ensures the conservation of the probability even in the $\mathcal{PT}$-broken regime as demonstrated in Fig. 3. This behavior is similar to that observed in single-particle open quantum systems [26], but it differs from the context considered here in time-dependent pseudo-Hermitian non-Hermitian systems, where the non-Hermitian term does not result from environmental effects, as in [26].

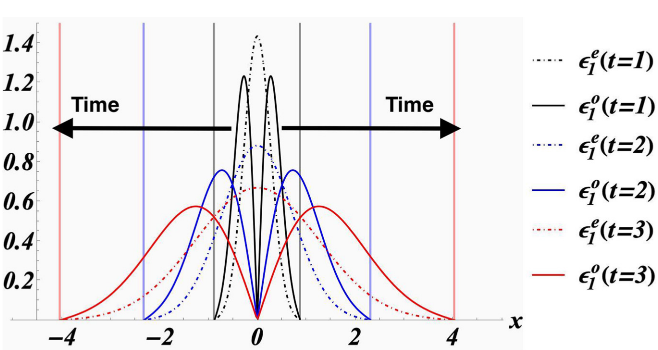

FIG. 3. Showing the infinite spreading of the probability density $\tilde{\phi}^\dagger\tilde{\phi}$ of the wave function (26) with time in $\mathcal{PT}$-broken regime. The vertical line is the boundary $\ell(t)$, which is found by solving the Ermakov-Pinney equation. In the $\mathcal{PT}$-symmetric regime, the boundary moves periodically with a similar spreading of the probability density.

IV. SWANSON MODEL: EQUIVALENCE OF TIME-DEPENDENT BOUNDARY AND DYSON MAP

This section illustrates the commutativity of the diagram shown in Fig. 1. Let us begin with the Swanson model (14). Performing the unitary transformation (5), the time-dependent non-Hermitian Hamiltonian is given in (6), where its explicit form is found to

$$i\hbar\partial_t\psi = -\frac{\omega_-\hbar^2}{2\ell^2}\psi_{yy} + \frac{\omega_+\ell^2}{2}y^2\psi + \hbar\mathcal{A}y\psi_y + \frac{\hbar\mathcal{A}}{2}\psi + \frac{\ell_t}{2\ell}\{y, i\hbar\partial_x\}\psi. \tag{27}$$

Similar to the previous section, we can perform further unitary transformations by $\psi = \exp(i\ell\partial_t\ell/2\hbar\omega_- y^2)\varphi(t, y)$ to the above equation. Let us consider the following Dyson map:

$$\eta = e^{-\frac{1}{2\hbar\omega_-}\mathcal{A}\ell^2y^2}, \tag{28}$$

$$\eta\psi = \eta e^{\frac{1}{2\hbar\omega_-}iLL_ty^2}\psi(t, y) = e^{\frac{1}{2\hbar\omega_-}(-\mathcal{A}L^2+iLL_t)y^2}\varphi(t, y), \tag{29}$$

which maps the non-Hermitian Hamiltonian to Hermitian Hamiltonian

$$i2\hbar\omega_-\ell^2\varphi_t + \hbar^2\omega_-^2\phi_{yy} - \ell^3(\Omega\ell + \ell_{tt})y^2\phi = 0. \tag{30}$$

Rescaling the variable as $y = \sqrt{\omega_-/2A_i}z$, the above equation is mapped to the effective Hamiltonian (21), rendering the equivalence of two approaches.

V. CONCLUSION

Our main finding is that time-dependent boundary conditions can be simulated with time-dependent metric operators and vice versa. In turn, this implies that the spontaneously broken $\mathcal{PT}$ regime can be mended, in the sense of acquiring real energies not only by a time-dependent metric, but equivalently also with time-dependent boundaries. We demonstrate our assertions for the exactly solvable pseudo-Hermitian Swanson model. For this model, the time-dependent boundary functions are restricted by the Ermakov-Pinney equation. The characteristic behavior of this function, which is periodic in time or divergent, is inherited by the time-dependent average of the energy function. These restrictions may be relaxed at the cost of the model no longer exactly solvable.

In the $\mathcal{PT}$-symmetric regime, we find an oscillatory behavior of the average energy similar to the one found in [11] for the harmonic oscillator with time-dependent coefficients. Different types of metric operators distinguish between whether this function has well-localized minima or maxima. In the spontaneously broken $\mathcal{PT}$ regime, the average energy is no longer periodic and develops only one well-localized minimum, irrespective of the choice of the metric.

ACKNOWLEDGMENT

T.T. is supported by JSPS KAKENHI Grant No. 22KJ0752.

[1] E. Fermi, Phys. Rev. **75**, 1169 (1949).
[2] S. Ulam, *Proceedings of the 4th Berkeley Symposium on Mathematical Statistics and Probability* (University of California Press, Berkeley, 1961), Vol. 3, pp. 315–320.
[3] G. M. Zaslavskiĭ and B. V. Chirikov, Sov. Phys. Usp. **14**, 549 (1972).
[4] A. Lichtenberg, M. Lieberman, and R. Cohen, Physica D **1**, 291 (1980).
[5] D. Gora and P. A. Collaboration, Universe **4**, 128 (2018).
[6] G. Karner, Lett. Math. Phys. **17**, 329 (1989).
[7] P. Seba, Phys. Rev. A **41**, 2306 (1990).
[8] S. Doescher and M. Rice, Am. J. Phys. **37**, 1246 (1969).
[9] A. Munier, J. Burgan, M. Feix, and E. Fijalkow, J. Math. Phys. **22**, 1219 (1981).
[10] D. Pinder, Am. J. Phys. **58**, 54 (1990).
[11] A. Makowski and S. Dembiński, Phys. Lett. A **154**, 217 (1991).
[12] P. Pereshogin and P. Pronin, Int. J. Theor. Phys. **32**, 219 (1993).
[13] V. Dodonov, A. Klimov, and D. Nikonov, J. Math. Phys. **34**, 3391 (1993).
[14] C. M. Bender and S. Boettcher, Phys. Rev. Lett. **80**, 5243 (1998).
[15] A. Mostafazadeh, J. Math. Phys. **43**, 205 (2002).
[16] F. Scholtz, H. Geyer, and F. Hahne, Ann. Phys. (NY) **213**, 74 (1992).
[17] M. S. Swanson, J. Math. Phys. **45**, 585 (2004).
[18] D. Musumbu, H. Geyer, and W. Heiss, J. Phys. A: Math. Theor. **40**, F75 (2007).
[19] A. Fring and T. Frith, Phys. Lett. A **381**, 2318 (2017).
[20] A. Fring, J. Phys.: Conf. Ser. **2448**, 012002 (2023).
[21] S. Di Martino, F. Anza, P. Facchi, A. Kossakowski, G. Marmo, A. Messina, B. Militello, and S. Pascazio, J. Phys. A: Math. Theor. **46**, 365301 (2013).
[22] A. Fring and M. H. Y. Moussa, Phys. Rev. A **94**, 042128 (2016).
[23] E. Pinney, *Proceedings of the American Mathematival Society* (AMS, Providence, RI, 1950), Vol. 1, pp. 681–681.
[24] V. P. Ermakov, Appl. Anal. Discret. Math. **2**, 123 (2008).
[25] J. V. José and R. Cordery, Phys. Rev. Lett. **56**, 290 (1986).
[26] N. Hatano and G. Ordonez, J. Math. Phys. **55**, 122106 (2014).